

Fluctuations of g -factors in metal nanoparticles: Effects of electron-electron interaction and spin-orbit scattering

Denis A. Gorokhov* and Piet W. Brouwer

Laboratory of Atomic and Solid State Physics, Cornell University, Ithaca, NY 14853-2501, USA

We investigate the combined effect of spin-orbit scattering and electron-electron interactions on the probability distribution of g -factors of metal nanoparticles. Using random matrix theory, we find that even a relatively small interaction strength significantly increases g -factor fluctuations for not-too-strong spin-orbit scattering (ratio of spin-orbit rate and single-electron level spacing $1/\tau_{\text{so}}\delta \lesssim 1$), and leads to the possibility to observe g -factors larger than two.

PACS numbers: 05.60.Gg, 72.25.Rb, 73.22.-f, 73.23.Hk

Electronic properties of metal nanoparticles can be studied on the single-electron level using “tunneling spectroscopy”, the measurement of the conductance of a metal particle coupled to source and drain electrodes via tunneling contacts [1]. These measurements have revealed important insights into the nature of the electronic ground and of individual excited states of normal metal, ferromagnetic, and superconducting nanoparticles [2, 3, 4, 5, 6]. Although tunneling spectroscopy involves processes in which only a single electron is added to or removed from the metal particle, the location of conductance peaks gives information about many-electron energy levels and, hence, about the role of electron-electron interactions.

The combination of electron-electron interactions and mesoscopic fluctuations of the density of states of a normal-metal nanoparticle can lead to a many-electron ground state with nontrivial spin $S = 1$, $S = 3/2$, or even larger [7, 8]. (Without interactions, the ground state spin is always $S = 0$ or $S = 1/2$.) In principle, the spin of a many-electron state $|k\rangle$ can be measured via the derivative of the energy E_k versus an applied magnetic field H , which is parameterized using the “ g -factor” g_k ,

$$\frac{\partial E_k}{\partial H} \bigg|_{H \rightarrow 0} = \pm \frac{1}{2} g_k \mu_B, \quad \mu_B = \frac{|e|\hbar}{2mc}. \quad (1)$$

If spin is a good quantum number, the positions of tunneling spectroscopy conductance peaks are unaffected by a nontrivial value of S , since tunneling spectroscopy measures differences of g -factors of many-electron states for which the electron number differs by one. Since the spin of a nanoparticle changes by $1/2$ upon addition or removal of an electron, all observed (differences of) g -factors are equal to two, irrespective of the individual g -factors of the two many-electron levels participating in the transition.

In this letter, we consider g -factor differences measured in tunneling spectroscopy in the presence of both

electron-electron interactions and spin orbit scattering. When spin and orbital degrees of freedom are coupled, randomness in the orbital part of wavefunctions is passed on to the spin part. Randomizing the electron spin lifts the “selection rule” that prohibited the observation of g -factors larger than two in the absence of spin-orbit scattering. It also leads to a decrease of g -factors, a suppression of the long-range exchange interaction (which is responsible for the high-spin states), and level-to-level fluctuations of g -factors [9, 10]. As we show here, selection rules are lifted already for a small spin-orbit scattering rate $1/\tau_{\text{so}} \lesssim \delta$, δ being the mean spacing between single-electron levels, whereas the decrease of g -factors and the suppression of the exchange interaction become effective at a larger spin-orbit rate $1/\tau_{\text{so}} \gtrsim \delta$ only, leaving a substantial parameter window where g -factor differences larger than two can be observed. Such large g -factors are a true many-electron phenomenon since, without interactions, all measured g -factors correspond to single-electron levels and are always ≤ 2 [11].

Model. Without interactions, the single-electron wavefunctions and energy levels of a metal nanoparticle are described by random matrix theory. With spin orbit scattering, the appropriate random matrix ensemble interpolates between the Gaussian Orthogonal Ensemble (GOE) and the Gaussian Symplectic Ensemble (GSE) [9],

$$H_0 = H_{\text{GOE}} + H_{\text{so}}. \quad (2)$$

Writing the spin degrees of freedom explicitly, one has

$$H_{\text{GOE}} = S \otimes \mathbb{1}_2, \quad H_{\text{so}} = \frac{\lambda}{\sqrt{4N}} \sum_{j=1}^3 i A_j \otimes \sigma_j,$$

where $\mathbb{1}_2$ is the 2×2 unit matrix in spin space, σ_j is the Pauli matrix ($j = 1, 2, 3$), S is an $N \times N$ real symmetric matrix, A_j is an $N \times N$ real antisymmetric matrix ($j = 1, 2, 3$), and $\lambda^2 = \pi/\tau_{\text{so}}\delta$ is the dimensionless spin-orbit scattering rate. The elements of the matrices S , A_1 , A_2 , and A_3 are drawn from independent Gaussian distributions with zero mean and with equal variances for the off-diagonal elements. The diagonal elements of S have double variance, whereas the diagonal elements

*e-mail: gorokhov@ccmr.cornell.edu

of A_1 , A_2 , and A_3 are zero because of the antisymmetry constraint. The limit $N \rightarrow \infty$ is taken at the end of the calculation. Each eigenvalue ε_μ of H_0 is doubly degenerate, with wavefunctions $\psi_{\mu 1}$ and $\psi_{\mu 2}$ related by time-reversal.

In normal-metal nanoparticles, the main contribution to electron-electron interactions is described by the “constant exchange interaction model” [12, 13],

$$H_{\text{ex}} = -J\mathbf{S}^2, \quad (3)$$

where \mathbf{S} is the total spin of the particle. The ratio of the exchange constant J and the mean spacing between single-electron levels δ corresponds to one of the Fermi Liquid constants of the metal. For most normal metals one has $0.2 \lesssim J/\delta \lesssim 0.4$, in agreement with electron-liquid theory [14], although smaller and larger values occur as well (see the discussion at the end of this letter). Combining the constant exchange interaction (3) and the single-electron Hamiltonian (2), and including the Zeeman coupling to a magnetic field \mathbf{H} in the z direction [11], one has

$$\hat{H} = \sum_\mu \varepsilon_\mu (\hat{\psi}_{\mu 1}^\dagger \hat{\psi}_{\mu 1} + \hat{\psi}_{\mu 2}^\dagger \hat{\psi}_{\mu 2}) - J\hat{\mathbf{S}}^2 - 2\mu_B H S_z, \quad (4)$$

where the first term comes from the diagonalization of the single-electron Hamiltonian (2).

If the number of electrons N_e is even, all many-electron states are non-degenerate in the presence of spin-orbit scattering. Hence all even-electron states have g -factors equal to zero. With spin-orbit scattering, odd-electron states are twofold degenerate (Kramers’ degeneracy). Since tunneling spectroscopy measures differences of g -factors for many-electron states with N_e and $N_e + 1$ electrons, a g -factor measured using tunneling spectroscopy is the g -factor of an odd-electron state if spin-orbit scattering is present. We assume that the nanoparticle relaxes to the even-electron ground state between tunneling events so that one measures g -factors of the odd-electron ground state and the odd-electron excited states upon increasing the bias voltage. In the (generic) case that the two tunneling contacts between the nanoparticle and the source and drain reservoirs have very different conductances, the height of a conductance peak is proportional to the matrix element [1]

$$w_k = \sum_{\sigma=\uparrow,\downarrow} |\langle N_e + 1, k | \hat{\psi}_\sigma^\dagger(\mathbf{r}) | N_e, 0 \rangle|^2, \quad (5)$$

where the creation operator $\hat{\psi}_\sigma^\dagger(\mathbf{r})$ creates an electron with spin σ in the grain at the position \mathbf{r} of the point contact with the smaller conductance, $|N_e, 0\rangle$ is the even-electron ground state, and $|N_e + 1, k\rangle$ is an odd-electron excited state. Without spin-orbit scattering, the weights w_k are zero for those states $|N_e + 1, k\rangle$ for which the spin

S_z differs by more than $1/2$ from the spin of the even-electron ground state $|N_e, 0\rangle$. (This is the “selection rule” referred to in the introduction.)

Limit of weak spin-orbit scattering. We first address the limit $\lambda \ll 1$, for which perturbation theory in λ is possible. In view of the above comments, we need to consider g -factors of odd-electron states only. For an odd-electron state $|k\rangle$ with spin $S = 1/2$ without spin-orbit scattering, spin-orbit scattering only affects the spin contribution to the g -factor to quadratic order in λ [15]. However, all nanoparticles have low-lying odd-electron states with spin $S = 3/2$ if the exchange interaction is present. (There even is a small but nonzero probability that the odd-electron ground state has spin $S = 3/2$ [7, 8].) Spin-orbit scattering lifts the fourfold degeneracy of an $S = 3/2$ odd-electron state and splits this state into two doublets. As we show below, spin-orbit scattering determines the g -factors of these doublets already to *zeroth* order in λ , whereas the matrix elements determining the corresponding tunneling spectroscopy peak height w_k are nonzero with finite probability.

Labeling the four members of the $S = 3/2$ quadruplet by the z component of the spin, $S_z = p - 5/2$, $p = 1, 2, 3, 4$, the matrix elements of H_{so} can be arranged in a 4×4 matrix V_k of the form

$$V_k = \begin{pmatrix} -a - d & b & c & 0 \\ b^* & -a + d & 0 & c \\ c^* & 0 & -a + d & -b \\ 0 & c^* & -b^* & -a - d \end{pmatrix}, \quad (6)$$

with a and d real numbers and b and c complex numbers. The specific form of (6) follows from time-reversal symmetry and guarantees that that the eigenvalues of V_k are doubly degenerate, in accordance with Kramers’ theorem. One has $V_k = 0$ to first order in H_{so} , since spin-orbit scattering does not mix states with opposite spin belonging to the same energy level. Calculating V_k to second order in H_{so} , we consider the special case when the $S = 3/2$ quadruplet is split by virtual transitions to one nearby odd-electron state $|l\rangle$ only. We refer to Ref. 16 for a general discussion; neglecting other states is justified if the energy difference of the virtual transition we consider is much smaller than other energy separations.

Since we are interested in g -factors only, it is sufficient to calculate the ratios b/d and c/d , for which we find

$$\begin{aligned} \frac{b}{d} &= \frac{(A_1 - iA_2)_{\mu\nu}(A_3)_{\mu\nu}\sqrt{3}}{(A_1)_{\mu\nu}^2 + (A_2)_{\mu\nu}^2 - 2(A_3)_{\mu\nu}^2}, \\ \frac{c}{d} &= \frac{(A_1 - iA_2)_{\mu\nu}^2\sqrt{3}}{(A_1)_{\mu\nu}^2 + (A_2)_{\mu\nu}^2 - 2(A_3)_{\mu\nu}^2}, \end{aligned} \quad (7)$$

where μ and ν refer to the two single-electron levels involved in the virtual transition. The $S = 3/2$ quadruplet splits into two doublets with g -factors g_{k1} and g_{k2} , with

$$g_{k1}^2 = 4 + \frac{12((A_1)_{\mu\nu}^2 + (A_2)_{\mu\nu}^2)}{(A_1)_{\mu\nu}^2 + (A_2)_{\mu\nu}^2 + (A_3)_{\mu\nu}^2},$$

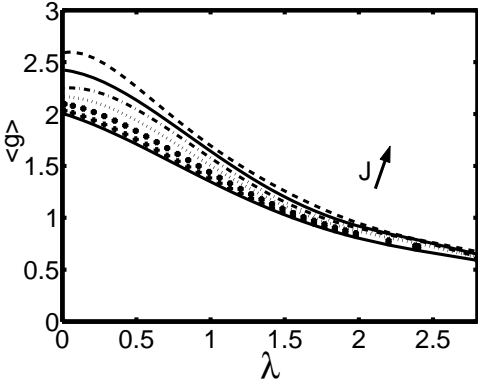


FIG. 1: Ensemble averaged g -factors for $J/\delta = 0, 0.1, 0.2, 0.3, 0.4, 0.5$, and 0.6 .

$$g_{k2}^2 = 48 - 3g_{k1}^2, \quad (8)$$

Whether g_{k1} or g_{k2} corresponds to the lower lying doublet depends on the relative position and spin of the virtual state; if the unperturbed $S = 3/2$ state is the ground state, the doublet with lower energy has g -factor g_{k1} [16]. Using the distribution of the matrices A_1 , A_2 , and A_3 , one finds that g_{k1} has the distribution

$$P_1(g_{k1}) = \frac{1}{2} \frac{g_{k1}}{\sqrt{48 - 3g_{k1}^2}}, \quad 2 \leq g_{k1} \leq 4. \quad (9)$$

The second g -factor g_{k2} takes values in the interval $0 \leq g_{k2} \leq 6$ and is related to g_{k1} via Eq. (8).

To zeroth order in λ , the tunneling spectroscopy peak heights (5) are nonzero if the even-electron ground state $|N_e, 0\rangle$ has spin $S = 1$. This occurs with significant probability for $J \gtrsim 0.3\delta$ [7, 8], so that the anomalous g -factors g_{k1} and g_{k2} are visible in a tunneling spectroscopy experiment with finite probability. Increasing the spin-orbit scattering rate λ further increases the visibility of peaks with the largest g -factors by mixing even-electron states with $S = 0$ and $S = 1$. Indeed, for $J = 0.3\delta$ the average energy difference between the lowest lying $S = 0$ and $S = 1$ even-electron states is $\sim \delta - 2J = 0.4\delta$, so that even moderate spin-orbit scattering ($\lambda \gtrsim 0.5\delta$) has a matrix element $\lambda\delta$ between the two states that is comparable with the energy difference. Inclusion of virtual excitations to other excited state changes the formulas for g_{k1} and g_{k2} , but not the conclusion that spin-orbit scattering affects the g -factors of the $S = 3/2$ states to zeroth order in λ .

Arbitrary spin-orbit scattering rate. In order to address the effects of a finite spin-orbit scattering rate, we have numerically diagonalized the Hamiltonian (4) for $0 < \lambda < 2.8$. We first diagonalized H_0 and considered the interaction H_{ex} in the basis of the 92 (76) lowest lying many-electron eigenstates of H_0 for N_e odd (even). We then diagonalized the remaining many-electron Hamiltonian and calculated the g -factors g_k of the $M = 8$ lowest-

lying odd-electron states, together with peak height w_k for transition from the even-electron ground state, see Eq. (5). The random matrices in our simulation are taken of size $2N = 400$ for $2 < \lambda < 2.8$ and of size $2N = 200$ for $\lambda < 2$. We averaged over 300 realizations of the random matrices, corresponding to a mesoscopic average over an ensemble of nanoparticles with equal size and spin-orbit scattering rate but different disorder configurations. In the analysis of the numerical data, we discarded all levels for which the peak height w_k is below a threshold w_{tr} , which we arbitrarily set at

$$w_{\text{tr}} = 0.1 \times \max_{k=1}^M w_k. \quad (10)$$

The threshold mimics the experimental reality that small peaks cannot be distinguished from the noise, and, hence, have their g -factors left out in the statistical analysis. Further, omitting g -factors for which $w_k < w_{\text{tr}}$ enforces the “selection rules” in the absence of spin-orbit scattering. We verified that the precise definition of w_{tr} does not affect our conclusions.

Interaction effects increase the ensemble averaged g -factor $\langle g \rangle$ significantly for $J \gtrsim 0.3\delta$ and $\lambda \lesssim 2$, see Fig. 1. In fact, there is a substantial parameter window for which $\langle g \rangle > 2$. By itself, such an increase of $\langle g \rangle$ has limited experimental relevance, since there is no independent method to measure λ . In fact, comparison of the measured $\langle g \rangle$ with theory is used to determine the spin-orbit rate $1/\tau_{\text{so}} = \lambda^2\delta/\pi$ in nanoparticles [5, 6]. This problem does not exist for the full (cumulative) probability distribution of g -factors (average and fluctuations), which is shown in Fig. 2. The values of J and λ in Fig. 2 are chosen such that all distributions have the same average $\langle g \rangle$. The distributions of Fig. 2, together with our numerical results for other values of J and λ (not shown), show that the exchange interactions substantially enhance the g -factor fluctuations (at the same value of the average). The probability $P(g > 2)$ to find a g -factor larger than two is shown in the inset of Fig. 2, as a function of J and λ .

Presently, g -factor distributions have been measured for the noble metals only [5, 6], for which $J/\delta \lesssim 0.1$ and interaction effects are negligible [17]. Indeed, the distributions measured in Refs. 5, 6 are in good agreement with the non-interacting theory [9, 10]. Interaction effects, nontrivial spin states, and, hence, g -factors larger than two should be observable for most other metals. For alkali metals, J/δ is in the range 0.2–0.3 [18], as well for Ti, Zr, and Mg [19, 20]. Even stronger interaction effects are expected for Nb, Rh, and Y nanoparticles, for which spin-density calculations set J/δ around 0.4 [21], and for Pt, Pd, and V, which have $0.6 \lesssim J/\delta < 1$ [22, 23]. For particles in the nm size range, spin-orbit effects are expected to be moderate or weak (dimensionless spin-orbit rate λ of order unity or smaller), except for the elements with the highest atomic numbers (Au, Pt). (Measured spin-orbit rates in Ag and Cu nanoparticles with radius

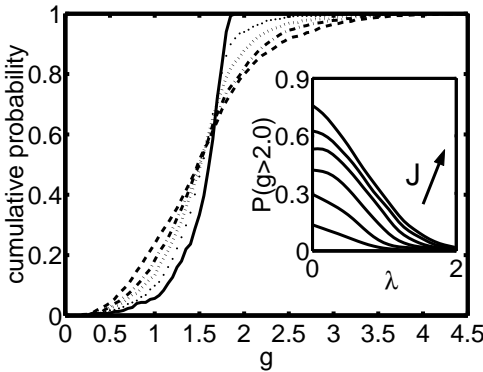


FIG. 2: Cumulative g -factor distribution for $\lambda = 0.70$, $J = 0$ (solid curve), $\lambda = 0.85$, $J = 0.2\delta$ (points), $\lambda = 0.90$, $J = 0.3\delta$ (dotted), $\lambda = 1.0$, $J = 0.4\delta$ (dash-dot), and $\lambda = 1.15$, $J = 0.6\delta$ (dashed). The values of λ are chosen such that $\langle g \rangle = 1.58$ in all cases. Inset: Probability for a level to have a g -factor larger than two, for $J/\delta = 0.1 - 0.6$, versus λ .

~ 4 nm were in the range $\lambda \sim 1$ [5].) For those elements for which spin-orbit effects are too weak to make large g -factors visible, spin-orbit scattering can be enhanced by doping with a small amount of, *e.g.*, Au atoms [24]. Similarly, doping with ferromagnetic atoms may increase J and drive the metals towards the Stoner instability at $J/\delta = 1$ [25].

In conclusion, we have shown that the presence of an exchange interaction with strength $J \gtrsim 0.2\delta$ leads to a significant broadening of the probability distribution of tunneling spectroscopy g -factors in normal metal nanoparticles. In particular, g -factors larger than two can be observed, which are a signature of non-trivial many-electron states. Weak spin-orbit scattering ($1/\tau_{\text{so}} \lesssim \delta$) is crucial in rendering the large g -factors observable, since it mixes many-electron states with different spin and, hence, lifts spin selection rules. It is only at larger spin-orbit scattering rates $1/\tau_{\text{so}} \gg \delta$ that spin-orbit scattering fully randomizes the spin and suppresses Zeeman contribution to g -factors and the matrix elements of the exchange interaction. The interaction range $J/\delta \gtrsim 0.2$ is appropriate for most metals, except for Al and the noble metals, which have negligible exchange interaction effects.

Whereas in gated semiconductor quantum dots the existence of nontrivial spin states could be inferred indirectly from the statistical distribution of Coulomb-blockade peak spacings [26], a comparison of the detailed parameter-dependence of successive peak positions [27], or from the succession pattern of g -factors of many consecutive levels [28], no such methods are available in metal nanoparticles without a gate or with a very limited gate voltage range. We hope that our finding that spin-orbit scattering renders nontrivial g -factors visible in standard tunneling spectroscopy without a gate motivates further experiments on metal nanoparticles with

strong interaction effects.

We thank S. Adam, A. Kaminski, A. H. MacDonald, J. R. Petta and D. C. Ralph for helpful discussions. This work was supported by the NSF under grant no. DMR 0086509 and by the Packard foundation.

- [1] J. von Delft and D. C. Ralph, Phys. Rep. **345**, 61 (2001).
- [2] C. T. Black, D. C. Ralph, and M. Tinkham, Phys. Rev. Lett. **76**, 688 (1996).
- [3] S. Guérón, M. M. Deshmukh, E. B. Myers, and D. C. Ralph, Phys. Rev. Lett. **83**, 4148 (1999).
- [4] D. Davidovic and M. Tinkham, Phys. Rev. Lett. **83**, 1644 (1999).
- [5] J. R. Petta and D. C. Ralph, Phys. Rev. Lett. **87**, 266801 (2001).
- [6] J. R. Petta and D. C. Ralph, Phys. Rev. Lett. **89**, 156802 (2002).
- [7] P. W. Brouwer, Y. Oreg, and B. I. Halperin, Phys. Rev. B **60**, 13977 (1999).
- [8] H. U. Baranger, D. Ullmo, and L. I. Glazman, Phys. Rev. B **61**, 2425 (2000).
- [9] P. W. Brouwer, X. Waintal, and B. I. Halperin, Phys. Rev. Lett. **85**, 369 (2000).
- [10] K. A. Matveev, L. I. Glazman, and A. I. Larkin, Phys. Rev. Lett. **85**, 2789 (2000).
- [11] In addition to the spin contribution to g factors there is an orbital contribution, which is predicted to give g factors larger than two in ballistic nanoparticles for strong spin-orbit scattering [10]. The orbital contribution it is small for diffusive nanoparticles and the spin-orbit rate $1/\tau_{\text{so}} \lesssim \delta$ we consider here. Moreover, no significant orbital contribution is found in experiments on ballistic noble metal nanoparticles [5, 6].
- [12] I. L. Kurland, I. L. Aleiner, and B. L. Altshuler, Phys. Rev. B **62**, 14886 (2002).
- [13] The other contribution is a “pairing interaction”, which, if attractive, causes a superconducting instability at sufficiently low temperatures. We consider normal metal nanoparticles for which the pairing interaction is small.
- [14] L. Hedin and S. Lundqvist, Sol. Stat. Phys. **23**, 1 (1969).
- [15] J. Sone, J. Phys. Soc. Japan **42**, 1457 (1977).
- [16] D. A. Gorokhov and P. W. Brouwer, unpublished (2003).
- [17] A. H. MacDonald, J. M. Daams, S. H. Vosko, and D. D. Koelling, Phys. Rev. B **25**, 713 (1982).
- [18] B. Knecht, J. Low Temp. Phys. **21**, 619 (1975).
- [19] I. Bakonyi, H. Ebert, and A. I. Liechtenstein, Phys. Rev. B **48**, 7841 (1993).
- [20] L. Wilk, W. R. Fehlner, and S. H. Vosko, Can. J. Phys. **56**, 266 (1978).
- [21] M. M. Sigalas and D. A. Papaconstantopoulos, Phys. Rev. B **50**, 7255 (1994).
- [22] E. Stenzel and H. Winter, J. Phys. F **16**, 1789 (1986).
- [23] F. Y. Fradin, D. D. Koelling, A. J. Freeman, and T. J. Watson-Yang, Phys. Rev. B **12**, 5570 (1975).
- [24] D. G. Salinas, S. Guérón, D. C. Ralph, C. T. Black, and M. Tinkham, Phys. Rev. B **60**, 6137 (1999).
- [25] For Pd, 3% of Ni doping is sufficient to create a ferromagnetic phase, see G. Chouteau, Physica B **84**, 25 (1976).
- [26] G. Usaj and H. U. Baranger, Phys. Rev. B **66**, 155333 (2002).

- [27] S. Lüscher, T. Heinzel, K. Ensslin, W. Wegscheider, and M. Bichler, Phys. Rev. Lett. **86**, 2118 (2001).
- [28] J. A. Folk, C. M. Marcus, R. Berkovits, I. L. Kurland, I. L. Aleiner, and B. L. Altshuler, Physica Scripta T **57**, 26 (2001).